



# Spectral and electrochemical solvatochromic investigations of newly synthesized peptide-based chemosensor bearing azobenzene side chain bio photoswitch

Petar Todorov<sup>a,\*</sup>, Stela Georgieva<sup>b</sup>, Petia Peneva<sup>a,d</sup>, Jana Tchekalarova<sup>c</sup>

<sup>a</sup> Department of Organic Chemistry, University of Chemical Technology and Metallurgy, 1756, Sofia, Bulgaria

<sup>b</sup> Department of Analytical Chemistry, University of Chemical Technology and Metallurgy, 1756, Sofia, Bulgaria

<sup>c</sup> Institute of Neurobiology, Bulgarian Academy of Sciences, 1113, Sofia, Bulgaria

<sup>d</sup> Institute of Mineralogy and Crystallography, Bulgarian Academy of Sciences, Sofia, 1113, Bulgaria

## ARTICLE INFO

### Keywords:

4-Aminoazobenzene  
Peptides  
Bio photoswitches  
Fluorescence spectroscopy  
Anticonvulsant activity  
Cyclic voltammetry

## ABSTRACT

In the present study, a novel analogue of azobenzene-containing hemorphin-4 has been synthesized and investigated for assessment of spectral, electrochemical, and biological effects. The synthesis was achieved by a modified solid-phase peptide synthesis (SPPS) by Fmoc-strategy. This compound represents a newly synthesized and unstudied peptide-based chemosensor bearing azobenzene side-chain with different spectral and electrochemical properties in the two *trans*-/*cis*-states depending on the solvent polarity. Their fluorescence intensity, as well as voltammetric behavior, was found to depend on both the polarity of the solvents and the type of isomers of the azopeptide compound. ~~The influence of the metal ions such as Zn<sup>2+</sup>, Ni<sup>2+</sup>, and Cu<sup>2+</sup> on the fluorescence emission intensity of *trans* forms in a water solution of the azopeptide has been also studied.~~ Both isomer forms have shown significant pH dependence, as the fluorescence peak and intensity are significantly distinguished in acidic and neutral medium. The electrochemical behavior before and after 90 min UV illumination was investigated using a cyclic voltammetric mode at three-electrode system with HMDE electrode as the working electrode.

The novel biopeptide Azo-Tyr-Pro-Trp-Thr-NH<sub>2</sub> was explored *in vivo* for potential anticonvulsant activity by 6-Hz seizure test and maximal electroshock test (MES) in ICR mice. The *cis*-Az-H4 isomer showed stronger potency than the *trans*-Az-H4 against both the 6 Hz-induced psychomotor seizures and tonic-clonic seizures in the maximal electroshock test with 100% protection demonstrated at the lowest dose of 1 μg administered intracerebroventricularly in mice. The effect of 1 and 5 μg *cis*-Az-H4 and 5 μg *trans*-Az-H4 was comparable to the positive control valproate in the 6-Hz test. None of the tested isomers displayed neurotoxicity in the rotarod test. Our results suggest that modified biopeptide in the N-terminus of hemorphin-4 with azobenzene deserve further exploration as a promising candidate with both anticonvulsant activity and as a chemosensor for pH determination.

## 1. Introduction

In recent years, azo-containing peptides are increasingly used due to their diverse physicochemical and biological properties. Often peptides containing chromophore units can recognize and respond to external stimuli. This exogenous influence is usually expressed, such as ligand binding, change in pH or temperature, or photon absorption can modulate the biomolecular structure to activate a biochemical signaling cascade of reactions. Nowadays, azo-containing peptides and their

analogues are used as biosensors and other biomedical applications [1–4].

The photodynamic control of peptide biomolecules can provide an easy and non-invasive way to study their effect or obtain a specific result by modulating the activity of the molecule [5,6]. The insertion of azobenzenes into peptides to photomodulate their conformational states was proposed firstly by Murray Goodman [7,8]. Azobenzene and its derivatives are the most widely used small-molecule chromophores, that possess interesting features [9]. Among them are photo-recording and

\* Corresponding author.

E-mail address: [pepi\\_37@abv.bg](mailto:pepi_37@abv.bg) (P. Todorov).

<https://doi.org/10.1016/j.dyepig.2021.109348>

Received 12 January 2021; Received in revised form 26 March 2021; Accepted 26 March 2021

Available online 31 March 2021

0143-7208/© 2021 Elsevier Ltd. All rights reserved.

photo-switching materials [10]. The presence of photo-inducible isomerism can be exploited in changing lipid membranes or to modulate the membrane interaction of peptides [10]. Also, they are applied for self-assembly processes as they show large changes in the molecule structure and properties in *trans-cis* photoisomerization [11–14]. Azobenzene-based biomolecular systems can also be easily manipulated with acid-base stimuli and photons, which makes them the subject of extensive research. The photoresponsive behavior is dependent on the pH and conformation of the azobenzene units. The physicochemical properties of the system are dependent on the mode of pH reduction and the isomeric *cis/trans* composition of the targets [15]. Increasing attention is being paid to water-soluble azobenzene derivatives synthesized for photo-regulation of functions and properties of biomolecules [16,17]. Nevertheless, water-soluble azobenzenes have been reported rarely and their properties, including the effect of pH and additives, are not understood well [18–20]. Azobenzene-containing peptides and photochromic compounds as a whole represent the basic molecular triggers for very important photo-regulated biological processes in living organisms [21,22]. The usage of azobenzene as a conformational model of peptide switching to control the conformational preferences of protein fragments by including different types of chromophores and various modes of their attachment have been described by Christian Renner and Luis Moroder [23].

The active demand of fluorescent materials with excellent properties and makings has led to the discovery of a newly phenomenon termed as aggregation-induced emission effect. In other words, organic chromophores emit more efficiently in the aggregate state than in solution [24]. Restriction of intramolecular rotation is the most commonly accepted mechanism for explaining this behavior [25].

Peptides with various optional building blocks, predictable conformations and high stability, are versatile and can act as tailor-made targeting probes for drug delivery [26]. Peptides with azobenzene moieties are very valuable as chemosensors because of their higher biological compatibility and solubility compared to organic dyes as well as stability compared to proteins in aqueous solutions [27]. The pH plays significant roles in biochemistry and medicine [28,29]. That's why methods for visualizing H<sup>+</sup> ions would be powerful tools to examine the concentration of H<sup>+</sup> ion signaling mechanisms in detail in different processes. For example, a highly pH-sensitive colorimetric chemosensor having a significant colour change would be very useful in the field of physiological fluids [30]. The pH-responsive molecules are based on varied electronic transfer effects turning in different tautomeric forms in a dependent manner from pH [20]. Peptide-based chemosensors have their modular nature, such as water solubility, biocompatibility, and low toxicity, high-affinity, and specific interactions with a target receptor [31–33]. Moreover, the peptide backbones can be synthesized by changing the amino acid sequences by the sophisticated solid-phase peptide synthesis (SPPS) technique and conjugated with different chromophores, including azobenzene derivatives [27].

Over the last decade, it has become clear that the degradation of cytosolic proteins can generate peptides that have biological activity. These include hemoglobin (Hb) peptides [34], which is a major component of red blood cells. Naturally occurring oxidants, such as hydrogen peroxide, modify Hb and generate denatured Hb, which is degraded by proteasomes and oligopeptidase to produce hemoglobin-active peptides. These are hemopressins and hemorphins, which can target mood-related receptors, such as cannabinoid and opioid receptors [35,36]. The first described hemoglobin-derived opioid peptide was hemorphin-4 (Tyr-Pro-Trp-Thr,  $\beta$ -chain 35–38), which has been isolated from bovine blood treated with a mixture of gastrointestinal enzymes [37].

Recently, a new analogue of hemorphin-5 containing azobenzene moiety was synthesized and characterized for its photophysical and electrochemical behavior by our group [38]. The results showed structure-activity relation to its E $\rightarrow$ Z photophysical properties activated by long-wavelength light at 365 nm. It was found that Z-isomer of

azo-peptide decrease the latency for onset of clonic seizures induced by intravenous pentylenetetrazole infusion test [38]. It should also be noted that so far, there are no data in the literature for the hemorphins containing azobenzene residue. Our previous investigation on a variety of newly synthesized hemorphin analogues that revealed promising pharmacological effects in mice provoked us further to explore their properties and future applications [39–43].

In this context, we have motivated our attention on the design and synthesis of the novel analogue of azobenzene-containing hemorphin-4 investigating its photophysical and electrochemical behavior in the both *trans-/cis*-states in different type of solvents as well as *in vivo* anticonvulsant activity of the two isomers. The structure-spectroscopic properties relationship has been also discussed.

## 2. Materials and methods

### 2.1. Synthesis of the peptide (Az-H4)

All reagents and solvents were analytical or HPLC grade and were bought from Fluka or Merck, and used without further purification. The protected amino acids and Fmoc (9-fluorenylmethoxycarbonyl)-Rink Amide MBHA (4-methylbenzhydrylamine) Resin were purchased from Iris Biotech (Germany). The 3-functional amino acids were embedded as follows: Tyr – as N $\alpha$ -Fmoc-Tyr (tBu)-OH, Thr – as N $\alpha$ -Fmoc-Thr (t-Bu)-OH, and Trp – as N $\alpha$ -Fmoc-Trp (Boc)-OH.

The solid-phase peptide synthesis by Fmoc strategy was used to obtain a new analogue of hemorphin-4 containing azobenzene moiety. The Fmoc-Rink-Amide MBHA resin (loading 0.71 mmol/g resin, cross linking 1% DVB) was used as solid phase carrier to obtain the C-terminal amide derivative and 2-(1H-benzotriazole-1-yl)-1,1,3,3-tetramethylammonium tetrafluoroborate (TBTU) was used as a coupling reagent. The coupling reactions were performed using for amino acid/TBTU/HOBt/DIEA/resin a molar ratio of 3/2.9/3/6/1, in a 1:1 mixture of DMF/DCM. A 20% piperidine solution in N,N-dimethylformamide (DMF) was used to remove the Fmoc group at every step. After each reaction step, the resin was washed with DMF (3  $\times$  1 min), isopropyl alcohol (3  $\times$  1 min) and CH<sub>2</sub>Cl<sub>2</sub> (3  $\times$  1 min). The coupling and deprotection reactions were checked by the Kaiser test [44,45]. The cleavage of the synthesized peptide from the resin was done, using a mixture of 95% trifluoroacetic acid (TFA), 2.5% triisopropylsilan (TIS) and 2.5% water. The peptide was obtained as a filtrate in TFA and precipitated with cold, dry ether. The precipitate was filtered, dissolved in water and lyophilized to yield the compound as a powder. The crude peptide was dissolved in H<sub>2</sub>O and acetonitrile was added until complete dissolving was observed. The peptide was obtained as a white powder with a purity of >97% as determined by analytical HPLC. The structure was confirmed by high-resolution electrospray mass spectrometry and NMR spectroscopy. The purity of the peptide was monitored on a reversed-phase high-performance liquid chromatography (RP-HPLC), column: Symmetry-Shield™ RP-18, 3.5  $\mu$ m, (50  $\times$  4.6 mm), flow: 1 mL/min, H<sub>2</sub>O (0.1% TFA)/CH<sub>3</sub>CN (0.1% TFA), gradient 0  $\rightarrow$  100% (45 min) and 100% (5 min). The crude peptide was purified using semi-preparative HPLC, column XBridge™ Prep C18 10  $\mu$ m (10  $\times$  250 mm), flow: 5 mL/min, H<sub>2</sub>O (0.1% TFA)/CH<sub>3</sub>CN (0.1% TFA), gradient 20  $\rightarrow$  100% (50 min).

The analytical data for the synthesized peptide prepared was as follows: t<sub>R</sub> 35.47 min, >97% pure, HRMS (ESI) calculated for C<sub>43</sub>H<sub>47</sub>N<sub>9</sub>O<sub>7</sub>, [MH<sup>+</sup>]: 801.8912; found: 802.3760.

The optical rotation in methanol (c = 0.01) at 20 °C was –14°.

<sup>1</sup>H NMR (600 MHz, DMSO-d<sub>6</sub>),  $\delta$  (ppm): 10.61 (s, 1H), 9.10 (s, 1H), 8.07 (d, J = 8.3 Hz, 1H), 7.84 (d, J = 7.4 Hz, 1H), 7.57–7.49 (m, 2H), 7.46 (d, J = 8.9 Hz, 2H), 7.36–7.25 (m, 4H), 7.23–7.18 (m, 1H), 7.07 (dd, J = 10.8, 8.0 Hz, 1H), 6.97 (d, J = 2.4 Hz, 1H), 6.93 (s, 1H), 6.90 (s, 2H), 6.82–6.65 (m, 2H), 6.45–6.38 (m, 2H), 6.36–6.32 (m, 2H), 4.42 (td, J = 8.9, 4.5 Hz, 1H), 4.34 (td, J = 7.6, 5.1 Hz, 1H), 4.17–4.11 (m, 1H), 3.92–3.78 (m, 2H), 3.56–3.45 (m, 2H), 3.34 (q, J = 8.5, 7.8 Hz, 2H), 2.96 (dd, J = 14.9, 5.1 Hz, 1H), 2.83 (dd, J = 14.9, 8.4 Hz, 1H),

2.63–2.53 (m, 1H), 2.50 (s, 2H), 2.42 (dd,  $J = 14.0, 9.4$  Hz, 1H), 2.27 (m, 2H), 1.54 (m, 2H), 1.04–0.98 (m, 2H), 0.76 (d,  $J = 6.5$  Hz, 3H).

$^{13}\text{C}$  NMR (151 MHz, DMSO- $d_6$ ),  $\delta$  (ppm): 172.51, 172.14, 171.77, 170.42, 169.42, 162.79, 156.32, 152.85, 152.18, 143.70, 136.49, 130.80, 130.06, 129.69, 128.05, 127.85, 125.35, 124.04, 122.27, 121.34, 118.80, 118.73, 115.39, 111.72, 110.37, 66.81, 59.99, 58.43, 54.33, 52.74, 47.25, 36.52, 36.26, 31.24, 27.42, 24.74, 20.43.

$^{13}\text{C}$  DEPT NMR (151 MHz, DMSO- $d_6$ ),  $\delta$  (ppm): 130.80, 130.06, 129.69, 125.35, 124.03, 122.27, 121.33, 118.80, 118.73, 115.56, 115.38, 112.48, 111.72, 66.81, 59.98, 58.42, 54.33, 52.74, 47.25, 36.52, 36.26, 31.23, 27.42, 24.74, 20.43.

Synthesis of the N-[4-(2-phenyldiazenyl)phenyl]glycine (3).

The compound (3) was synthesized from 4-aminoazobenzene (1) by the adapted methodology according to the previously described method for the synthesis of aminoazobenzene derivatives [14,46].

## 2.2. Physicochemical characterization

### 2.2.1. Spectral measurements

A double-beam UV-Vis “Varian-Cary” with 1 cm path length synthetic quartz glass cells spectrophotometer was used for absorption spectra recording. The fluorescence spectra were recorded on a PerkinElmer LS55 spectrophotometer at the same concentrations. The solvents (spectroscopic grade) used in this study were: dimethyl sulfoxide (DMSO), acetonitrile (AcCN) and phosphatic buffer solution (pH 6.86). The concentrations of the compounds in the spectral solutions are as follows: Az-H4:  $C = 1.04 \times 10^{-5}$  mol L $^{-1}$  (concentration of stock solution of Az-H4:  $C = 4.68 \times 10^{-3}$  mol L $^{-1}$  in DMSO); N-[4-(2-phenyldiazenyl)phenyl]glycine (Az):  $C = 1.754 \times 10^{-5}$  mol L $^{-1}$ . The effect of the metal cations as well pH of the aqua solution upon the fluorescence intensity of both cis(Z)- and trans(E)- isomers was also examined by preparation of solution with an equal concentration of azo peptide compound ( $C = 1.04 \times 10^{-5}$  mol L $^{-1}$ ) in the presence of certain amounts of metal solutions as follows: 50.0  $\mu\text{L}$  of stock solution of the metal cations (concentration of stock solution of:  $\text{Cu}^{2+}$  ( $C = 1.14 \times 10^{-2}$  mol L $^{-1}$ ); 100.0  $\mu\text{L}$   $\text{Zn}^{2+}$  ( $C = 1.23 \times 10^{-2}$  mol L $^{-1}$ ); 50.0  $\mu\text{L}$   $\text{Ni}^{2+}$  ( $C = 1.14 \times 10^{-2}$  mol L $^{-1}$ ) and HCl, respectively. All used reagent were analytical grade.

The spectrum was recorded in potassium bromide (KBr) pellet with a Varian 660 FTIR spectrophotometer the spectra in the range 4400–600  $\text{cm}^{-1}$  using a Fourier Transform Infrared Spectroscopy (FT-IR). The sample was scanned 256 times with a resolution of 2  $\text{cm}^{-1}$  and signal-averaged for each sample in the range of 400–4000  $\text{cm}^{-1}$ . The first and second derivatives of the absorption spectrum were performed by Savitsky-Golay with polynomials derivation of convolution coefficients 2 and smoothing factor 40.

The NMR spectra were recorded on a Bruker Avance II + spectrometer operating with frequency 600 MHz for  $^1\text{H}$  and 125 MHz for  $^{13}\text{C}$  in DMSO- $d_6$ . Chemical shifts  $\delta$  are reported in ppm, and coupling constants  $J$  are reported in Hz.

The molecular mass and purity of the compound was confirmed by high-resolution electrospray mass spectrometry on a Q Exactive high-resolution mass spectrometer (Thermo Fisher Scientific Inc., USA) equipped with TurboFlow TM Transcend chromatography system (Thermo Fisher Scientific Inc., USA) and heated electrospray ionization (HESI II) source. Data acquisition and processing were done by XCalibur® 2.4 software (Thermo Fisher Scientific Inc., USA). The instrumental parameters were as follows: Spray Voltage – 4.0 KV, Sheath Gas – 30 AU, Auxiliary Gas – 12 AU, Capillary Temperature – 300 °C, Spare Gas – 3 AU, Heater Temperature – 300 °C. Full scan experiments were carried out in a range of 120–2000  $m/z$  at 140 000 resolution.

Optical rotations were recorded on an MCP200 modular circular polarimeter (Anton Paar Opto Tec GmbH, Seelze, Germany).

## 2.3. Electrochemistry

### 2.3.1. Apparatus

A voltamperometric analyzer (Metrohm-797VA) in connection with VA-stand 797 (Metrohm) was used with the three-electrode system consisting of HMDE as a working electrode (areas of 0.030  $\text{cm}^2$ ), Ag|AgCl|3 M KCl as a reference electrode, and carbon as an auxiliary electrode. Electrochemical data processing were performed by Origin-Pro 8.0 software.

### 2.4. Procedures

Measurements were carried out at room temperature (25 °C). Azo-peptide before and after UV illumination at 365 nm was adsorbed on the electrode from stirred solutions for a 30 s deposition time at  $-1.2\text{V}$ . The voltamperograms were recorded after 200s purging with argon from 0.3 to  $-1.4$  V at a 1.00 V/s scan rate and 0.010 V voltage step in cyclic voltammetric mode. For an investigation of the ratio of scan rate vs. current intensity, a concentration from  $6.68 \times 10^{-5}$  mol L $^{-1}$  of Az-H4 was used. An aliquot of stock solution of Azo-peptide before and after 90 min UV illumination at 365 nm was placed in a 10 mL-electrode cell containing 7 mL electrolyte and the signals were recorded.

## 2.5. Biology. In vivo experiments

### 2.5.1. Animals and treatment

ICR male adult mice (25–30 g), delivered from the animal facility of the Institute of Neurobiology, Bulgarian Academy of Sciences, were accommodated under standard conditions as follows: room temperature  $21 \pm 2$  °C, relative humidity, light/dark (12/12) regime, plexiglass cages in groups of 3–4 with water and food *ad libitum*. The peptide analogues were suspended in saline. All procedures were performed in agreement with the European Communities Council Directive 2010/63/EU.

## 2.6. Drugs and dosage

The mice were infused intracerebroventricularly (i.c.v.) (10  $\mu\text{L}$ /ventricle) at doses of 1, 2.5 and 5  $\mu\text{g}$ /mouse by means of 28-gauge stainless steel needle attached to a 10- $\mu\text{L}$  Hamilton® syringe as described previously [42]. The injection needle was left in place for 2 min to avoid back diffusion of the solution. Ten min following the injection procedure, the test for anticonvulsant activity or neurotoxicity was evaluated.

## 2.7. Anticonvulsant activity

### 2.7.1. Maximal electroshock test (MES test)

MES test was performed as described previously [42]. Tonic-clonic seizures in controls were produced by corneal electrical stimulation (50 mA, 60 Hz, 0.2 s) via Constant Current Shock Generator. The lack of hind limb tonic extension of the tested mouse was accepted as a criterion for anticonvulsant activity of the tested compound. Each mouse was used only once.

### 2.8. 6-Hz psychomotor seizure test

The corneal stimulation with 32 mA, 6 Hz for 3 s was applied as described earlier [42]. The electric stimulus of 32 mA, 6 Hz for 3s was conducted via corneal electrodes for evaluating the efficacy of the compounds against psychomotor seizures. The responses in control mice are characterized by a minimal clonic seizures, stereotyped behaviors, twitching of the vibrissae or Straub-tail. The criterion for seizure suppression is accepted when the tested mouse resumes normal position 10 s after stimulation.

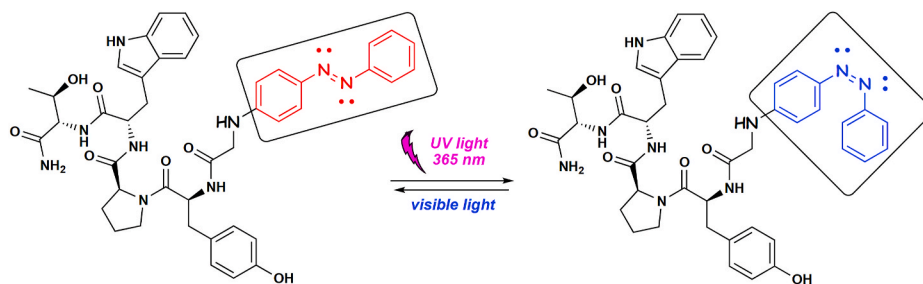
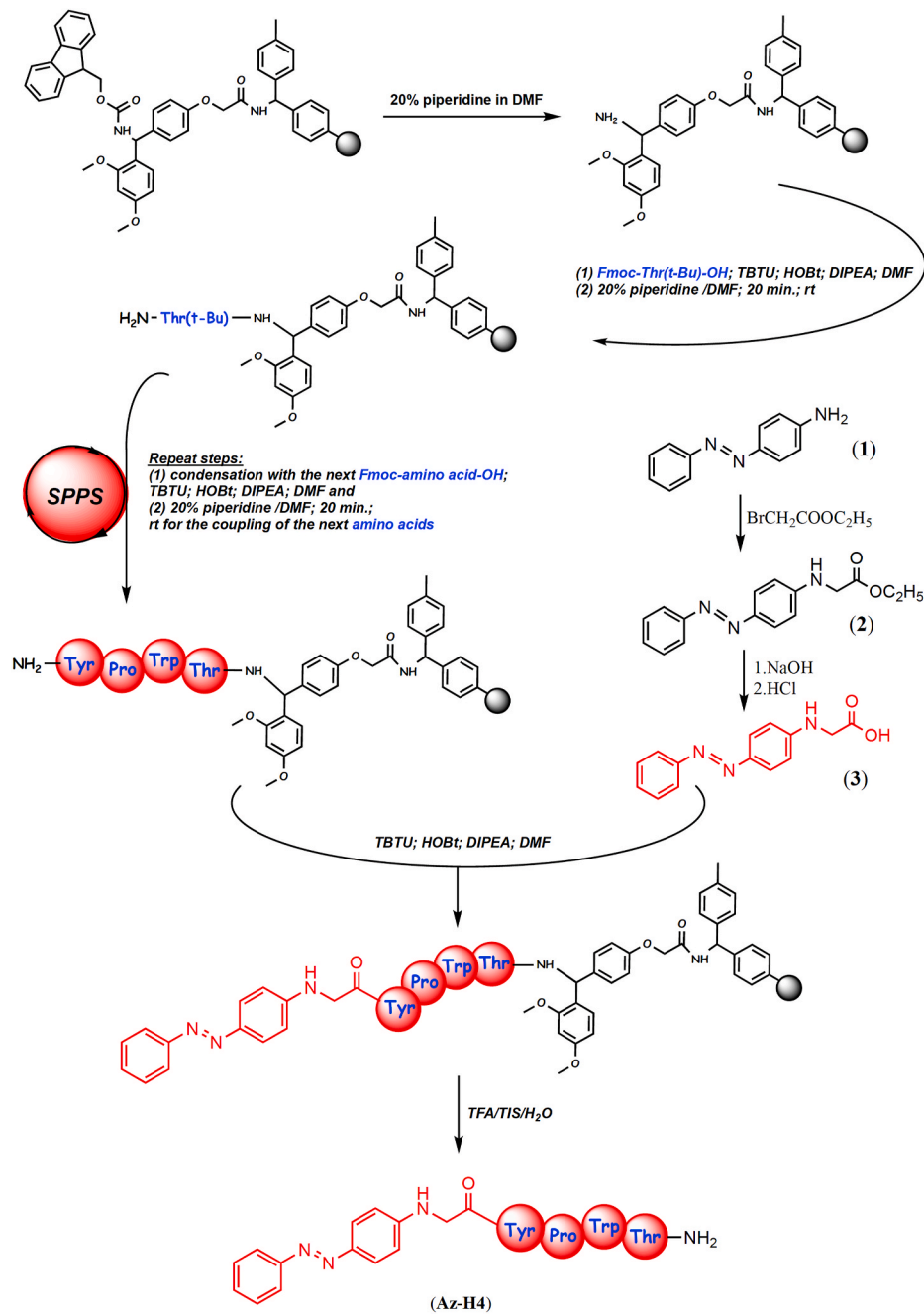


Fig. 1. Schematic representation of photoswitchable Azo-Tyr-Pro-Trp-Thr-NH<sub>2</sub> (Az-H4) peptide upon long wavelength UV light as *trans* (*E*) and *cis* (*Z*) isomers. The azobenzene photoswitch moiety is highlighted as red/blue.



Scheme 1. Synthetic pathway of the azobenzene-containing hemorphin-4 (Az-H4).

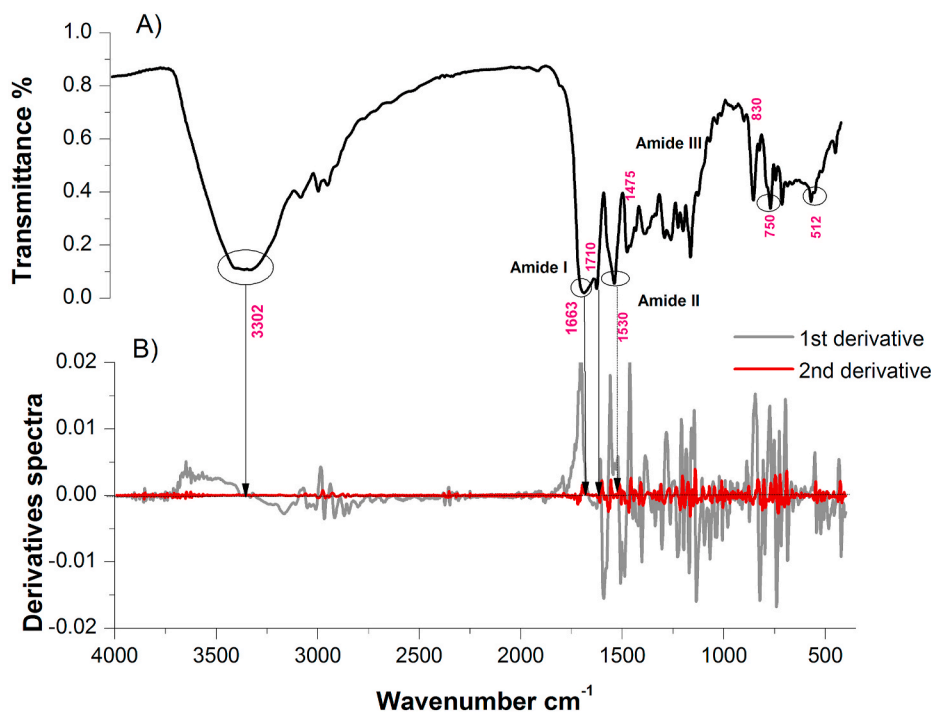


Fig. 2. Zero order (A) and first and second derivative (B) IR spectra of the azopeptide Az-H4 compound; characteristic regions for peptide moiety: Amid A: 4000–2600  $\text{cm}^{-1}$ , Amid I: 1600–1700  $\text{cm}^{-1}$ , Amid II: 1528–1577  $\text{cm}^{-1}$  and Amid III at 1221–1331  $\text{cm}^{-1}$  [55].

## 2.9. Rotarod test

The neurotoxicity was assessed as described previously in a rotarod apparatus for mice [42]. The tested mouse was placed on a rotating rod (3.2 cm in diameter, at a speed 10 rpm). The compound that causes a loss of coordination of the tested mouse and inability to keep a position on the rod for at least 1 min from the three possible sessions trials was accepted as neurotoxic.

## 2.10. Statistical analysis

Fisher's exact was used for the analysis of data from MES and 6-Hz test. Statistical significance was accepted at  $p < 0.05$ . The calculations were carried out with Graph Pad Prizm Version 7.04 (GraphPad Software, San Diego, CA, USA.) and Sigmapstat (version SigmaStat® 11.0) for Windows.

## 3. Results and discussion

### 3.1. Chemistry

In view of the above mentioned the main goal in this research is to synthesis and investigate the spectral, electrochemical and biological effects of new biopeptide bearing azobenzene to the N-side chain of hemorphin-4 obtaining azo-peptide Az-H4 (Fig. 1).

For the preparation of Az-H4 firstly it needs to be synthesized N-[4-(2-phenyldiazenyl)phenyl]glycine (3). Unfortunately, only a few protocols for obtaining N-[4-(2-phenyldiazenyl)phenyl]glycine have been reported [14,46]. The compound (3) incorporated in biomolecular systems are capable of recognizing and responding to external stimuli such as ligand binding, a change in pH or temperature, or absorbance of a photon etc. [3]. As a potential fragment for pharmaceutical and many other research and development applications, finding a general and improved method to synthesize N-[4-(2-phenyldiazenyl)phenyl]glycine analogues is essential [2,3,47–49]. The starting compound (3) used to obtain the desired compound Az-H4 was synthesized from 4-aminoazobenzene (1) under the influence of ethyl bromoacetate in the medium of

absolute ethanol (Scheme 1) to give the ethyl (E)-(4-(phenyldiazenyl)phenyl)glycinate (2). After that, the alkaline hydrolysis of 2 with NaOH followed by acidification with HCl yielded compound 3 (Scheme 1). The azo-peptide (Az-H4) was prepared by solid-phase peptide synthesis (SPPS)-Fmoc (9-fluorenylmethoxy-carbonyl) chemistry using TBTU (2-(1H-benzo-triazole-1-yl)-1,1,3,3-tetramethyluronium tetrafluoro-borate), an efficient peptide coupling reagent (Scheme 1). The SPPS, based on the reaction of N-[4-(2-phenyldiazenyl)phenyl]glycine (3) with N-terminal amino group of Tyr-Pro-Trp-Thr tetrapeptide directly on the resin. After cleavage of the product from Rink-Amide MBHA Resin by TFA to give the Az-H4, the azo-peptide was purified from crude product by semi-preparative HPLC with a C18 column. The molecular weight was determined, using HRMS (ESI). The structure of the obtained compound was checked by UV-Vis, IR, NMR ( $^1\text{H}$ ,  $^{13}\text{C}$ , DEPT) spectra. The analytical data are presented in the Material and Methods Section.

### 3.2. Spectral characterization

#### 3.2.1. IR spectroscopy

The determination of the type of the secondary peptide structure is essential for the study of some physicochemical characterizations of the molecule such as the solubility of the molecule, its passage through biological membranes as well acid/base (pKa) constant determination and etc. To check whether the azo component changes the type of structure of the peptide bone and vice versa whether the peptide influence the maxima and intensity of the azo component, IR spectra in the range 4000–350  $\text{cm}^{-1}$  were recorded. The frequency maxima of the azo group range from 1500 to 1630 depending on the type of the azo compound and the functional groups and its participation in different structural conjugations [52]. In the case of asymmetric azo derivatives, the vibration of the  $-\text{N}=\text{N}-$  bond in some azo compounds between 1630 and 1575  $\text{cm}^{-1}$  could not be observed [53,54]. In the mentioned above one can find the spectral characterization regions for peptide structure indicated as follows: Amide I, II, and III (Fig. 2). In Fig. 2 are also given the zero and derivatives (1st and 2nd) spectra of the Az-H4 compound for more clearly distinguish the absorption maxima. Our data show a

**Table 1**

Basic photophysical characteristics of the isomers of a compound Az-H4 and Az-H4(IRr) in solutions with different polarity.

Compound/solutions		DMSO	AcCN	H <sub>2</sub> O	0.1 M HCl
Az-H4	$\lambda_{abs.}$ (nm)	410	395	391	513
	$\lambda_{emi.}$ (nm)	468	457	436	555
	$\epsilon \cdot 10^4$ (L mol <sup>-1</sup> cm <sup>-1</sup> )	2.01	4.21	3.12	3.27
	Stokes offset (nm)	58	62	45	42
Az-H4(IRr)	$\lambda_{abs.}$ (nm)	410	395	391	508
	$\lambda_{emi.}$ (nm)	470	456	437	554
	$\epsilon \cdot 10^4$ (L mol <sup>-1</sup> cm <sup>-1</sup> )	2.13	4.56	3.07	3.16
	Stokes offset (nm)	60	61	46	46

broad absorption maximum in the high-frequency region (3600–2860 cm<sup>-1</sup>) corresponding to valence vibrations at NH<sub>3</sub><sup>+</sup> group ( $\nu_{NH_3^+}^{as}$ ) (Fig. 2). The frequency maxima localized at 3302 cm<sup>-1</sup> could be attributed to N–H stretching vibration ( $\nu_{NH}$ ) (Amid A) [43]. Between the wavenumber values from 1610 to 1663 cm<sup>-1</sup>, a high-intensity spectral band split in two is observed. The peak at 1663 cm<sup>-1</sup> is due to vibration of  $\nu_{C=O}$  (Amide I) [43] and that at 1610 cm<sup>-1</sup> generally could be assigned to vibration of –N=N– group. The  $\delta_{NH}$  vibration of Amide II band is appeared at about 1530 cm<sup>-1</sup> and fully corresponding to reported in the literature high absorbance maximum of amide spectrum which proposes  $\beta$ -turn or  $\beta$ -sheet secondary structure of the peptides [55]. In addition, the characteristic bands of the Amide III region are clearly visible on the IR spectrum localized at 1236 cm<sup>-1</sup> and 1176 cm<sup>-1</sup> (Fig. 2). The short peptide backbone as well appearing of amino acids such as Tyr and Trp in the structure of investigated peptides prevent the helical folding of the peptide and hence the existence of an alpha helix [55]. Substitution of Pro and presence of azo component on the peptide

chain also suppose the possibility of a beta-structure existing and breaking down of an alfa-helix conformation.

### 3.2.2. Photophysical properties

The main absorption and emission characteristics of the synthesized compound before and after 90 min UV illumination at 365 nm were studied in solutions with different polarity, increasing in the order: DMSO < AcCN < H<sub>2</sub>O and are presented in Table 1. The spectrum in the visible region were compared with the spectrum of starting azo compound (Figs. 3 and 4).

The absorptions spectra are presented in Fig. 3 by means of zero-order and derivative spectra. Differentiation of the absorption signals was necessary in order to enhanced resolution and more readily appreciated more complex spectra. The UV–Vis spectra of Az-H4 and free from peptide azo component give clearly shaped different intensity absorbance bands localized at  $\approx$ 400 nm which could be attributed to –N=N– group with  $n \rightarrow \pi^*$  energy transition. As the polarity of the solvent increases, a bathochromic shift of the signal in the UV spectrum is observed, showing positive solvatochromism. Compared to the starting azo compound, it can be seen that the solvatochromic properties of the hybrid peptide are mainly due to the azo component, as the colour change of the solution with increasing solvent polarity does not differ from that reported in the azo compound literature [56,57]. The binding with peptide moiety increases the absorbance of Az-H4 in all investigated mediums, the most strong is in acetonitrile (Fig. 3). Basically the  $\pi \rightarrow \pi^*$  transitions of the >C=O in the peptide bonds is occurs by UV absorption of the peptide molecule in the range 180–230 nm. Both Trp and Tyr are primarily responsible for the inherent absorption of the peptides at higher wavelengths: absorption at 285 nm is dominated by the  $\pi$ -electron systems of aromatic side-chains of indol of Trp and phenol

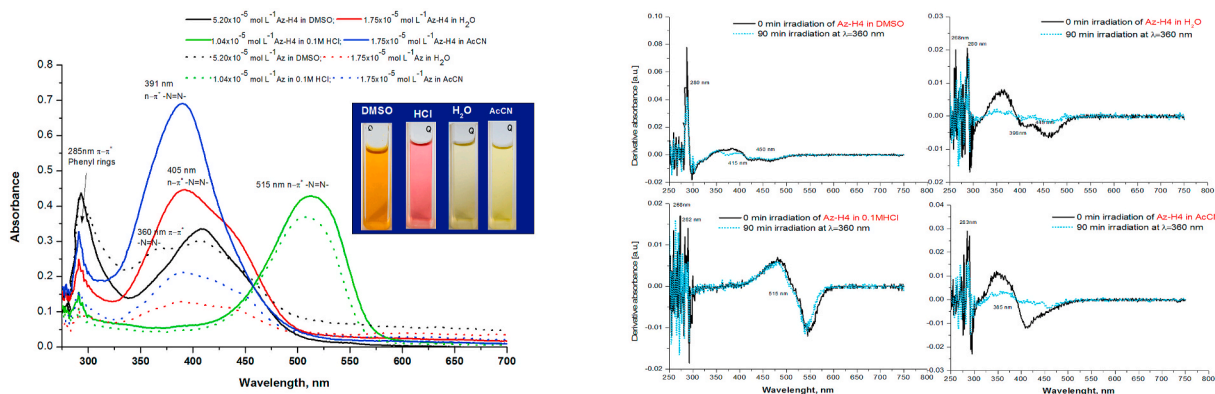


**Fig. 3.** UV-VIS spectra of the Azo-Tyr-Pro-Trp-Thr-NH<sub>2</sub> (Az-H4) and N-[4-(2-phenyldiazenyl)phenyl]glycine (Az) in different solvents ((left) and first derivatives spectrum before and after 90 min UV-illumination with 365 nm (right)).

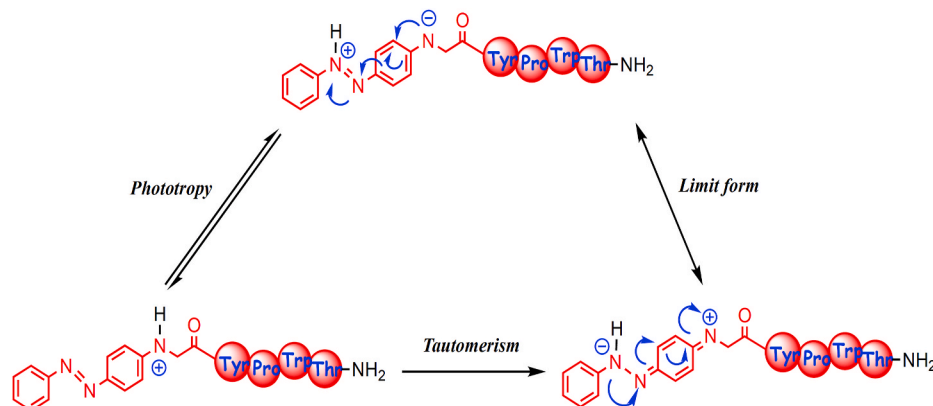


**Fig. 4.** Ammonium-azonium tautomerism of the Az-H4 compound in the presence of protonic solvent (0.1 M HCl) [52].

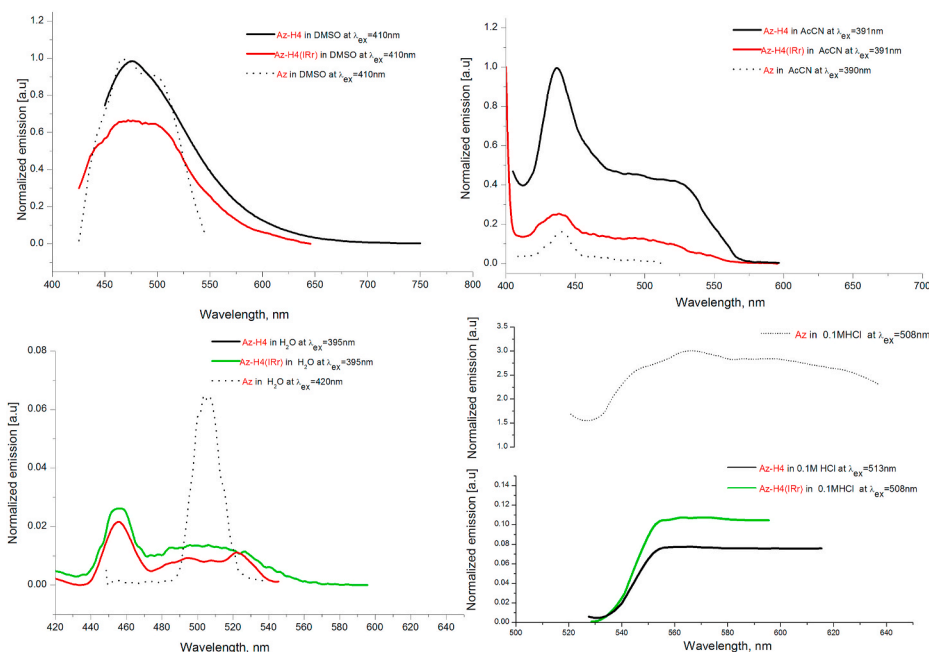


**Fig. 5.** Emission/fluorescence spectra of N-[4-(2-phenyldiazenyl)phenyl]glycine (Az) and Azo-Tyr-Pro-Trp-Thr-NH<sub>2</sub> (Az-H4) and after 90 min UV illumination at  $\lambda = 365$  nm (Ar-H4(IRr) in different solvents; concentration of all analyte solutions:  $5.20 \times 10^{-5}$  mol L<sup>-1</sup>.

ring of Tyr [58,59]. The more evident signals, especially in the range of 270–300 nm, could be observed on the derivatives graphics. One can see that the derivative spectra indicate three bands related to the phenylazo part, Tyr and Trp. After UV illumination with 365 nm for 90 min, the Tyr and Trp as well for  $\pi \rightarrow \pi^*$  of  $-N=N-$  absorption increased due to basically of the conformation changing.

In the presence of hydrochloric acid, the absorption spectrum is changed (Fig. 3). The addition of hydrochloric acid shifts the maximum at  $\approx 400$  nm of both isomers to longer wavelengths - 513 nm for *trans* (*E*-

and 508 nm for *cis* (*Z*)- form, respectively, and changed the colour of the solution which indicates the conversion of azo group into a protonic form and suppose better solvation of each form of the compound in water solutions [52]. The influence of proton-saturated medium and the possibility for the intramolecular migration of the proton from one element to another gives resonance-stable ammonium-azonium tautomerism of the azopeptide structure and following different colour of the solution (Fig. 4).

The dyes exhibit complex spectral behavior, which strongly depends

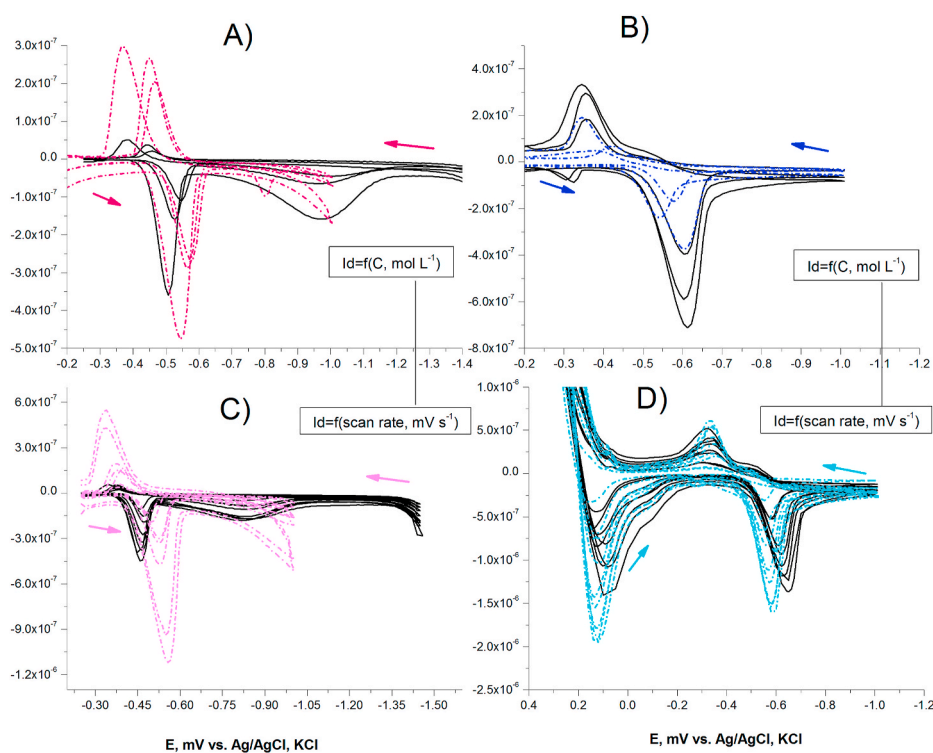


**Fig. 6.** Cyclic voltammograms of Az-H4 and Az-H4 (IRR) in different electrolyte media, scan rate and concentration using HMDE and Ag/AgCl, KCl as reference electrode: A) CVs of Az-H4 and Az-H4 (IRR) (in colour) at different concentrations: from  $1.67 \times 10^{-5}$  to  $6.681 \times 10^{-5}$  mol L<sup>-1</sup> in pH 6.86 (phosphate buffer solution, 0.1 mol L<sup>-1</sup>), scan rate 1.00 V s<sup>-1</sup>; B) CVs of Az-H4 and Az-H4 (IRR) (in colour) at different concentrations:  $1.67 \times 10^{-5}$  to  $6.681 \times 10^{-5}$  mol L<sup>-1</sup> in AcCN; C) Cyclic voltammograms of  $6.681 \times 10^{-5}$  Az-H4 before and after (in colour) UV illumination in pH 6.86 (phosphate buffer solution, 0.1 mol L<sup>-1</sup>) at different scan rate from 0.2 to 2.0 V s<sup>-1</sup>; D) Cyclic voltammograms of  $6.681 \times 10^{-5}$  Az-H4 before and after (in colour) illumination in AcCN at different scan rate from 0.2 to 2.0 V s<sup>-1</sup>.

**Table 2**

Voltamperometric characteristic of Az-H4 before and after (Az-H4 (IRr)) UV irradiated with  $\lambda = 365$  nm at concentration  $6.681 \times 10^{-5}$  mol L<sup>-1</sup> in different electrolyte media at HMDE electrode; heterogen rate constant and diffusion coefficient of Az-H4 and Az-H4(IRr) at HMDE electrode (with electrode area, A = 0.030 cm<sup>2</sup>).

Compound/ electrolyte	$-E_{pc}$ , V	$E_{pa}$ , V	$E_{pc}$ - $E_{pa}$ / 2 mV	$-I_{pc}$ , A	$I_{pa}$ , A	Nature of the reduction process	$k_{sh}^0$ $\times$ $10^{-4}$ cm s <sup>-1</sup>
Az-H4/Ph. buffer (pH 6.86)	0.547	0.458	18	1.02 $\times$ $10^{-7}$	2.16 $\times$ $10^{-8}$	R <sup>a</sup>	0.692
Az-H4(IRr)/ Ph.buffer (pH 6.86)	0.573 0.801	0.464 -	20	2.73 $\times$ $10^{-7}$ 7.16 $\times$ $10^{-8}$	2.07 $\times$ $10^{-7}$ -	R	2.01
Az-H4/ AcCN	0.603	0.355	28	3.67 $\times$ $10^{-7}$	1.66 $\times$ $10^{-7}$	R	1.97
Az-H4(IRr)/ AcCN	0.603	0.345	25	3.52 $\times$ $10^{-7}$	1.76 $\times$ $10^{-7}$	R	2.14

<sup>a</sup> R-reversible; n-number of electron exchanged of  $-N=N-$ .

on the properties of the solvent. Fluorescence spectroscopy was used to study the solvatochromic behavior of the azopeptide. The spectrum before and after 90 min UV illumination at 365 nm of Az-H4 in four solvents with different polarity: DMSO; H<sub>2</sub>O, HCl and AcCN are given on Fig. 5. In both cis (Z)- and trans (E)- isomerization the compound has an intense colour which is changed depending on the polarity of the solvent from yellow/orange (DMSO, AcCN, H<sub>2</sub>O) to red (HCl). Their absorption maxima basically depend on the type of protonic solvent due to the ongoing tautomerism affecting the azo group in a solution saturated

with protons such as HCl-solution and are respectively at 395 nm in H<sub>2</sub>O, 391 nm in AcCN, 410 nm in DMSO. A bathochromic shift of the maximum in the order AcCN, H<sub>2</sub>O < DMSO < HCl as well a hypochromic effect in the organic solvents when the compound is irradiate are observed which could be attributed to the relation of intramolecular interactions and conformational states changed of the compounds. The type of absorption and emission maxima is also influenced by the peptide sequence associated with the azo component. This statement is confirmed by the fact that as a result of intramolecular changes of the compound due to the presence of photosensitive groups of amino acid fragments displace and mainly increase the absorption and emission intensity of the azo compound. It is known that the amino acid residues: Tyr, Phe, and Trp the peptides possess a fluorescence in UV range [38] and the energy absorbed by Phe and Tyr is often transferred to the Trp, because of their spectral properties, resonance energy occurs from Phe to Tyr to Trp [38]. Typically for the investigated compound containing amino acid sequence -Trp-Pro-Tyr- is that this structural unit suggests a trans configuration of Tyr and Trp residues around Pro. The excitation/emission spectra of azopeptide compound with similar peptide bone has been studied in our previous work where was proved that the indole from Trp is highly sensitive to polarity, local environment and conformational changes [38]. Moreover, the energy transfer from Tyr to Trp is very sensitive to the conformational changes because it is realized close to the trans configuration.

The differences between the structure and functional properties of the azopeptide compound in its excited (S1) and ground (S0) states before and after UV illumination at 365 nm were assessed by the value of the Stokes shift in nm. The calculated values of the Stokes offset are also given in Table 1. As the polarity of the solvents increases, the influence of the tautomerization in Az-H4 compound shows lower energy of  $\lambda_{max}$  and a high molar extinction coefficient, which is an indication of the course of intramolecular charge transfer during the transition to the excited state.

From a biological point of view, the interaction of metals with Az-H4 in a medium close to the physiological is important to be studied in order

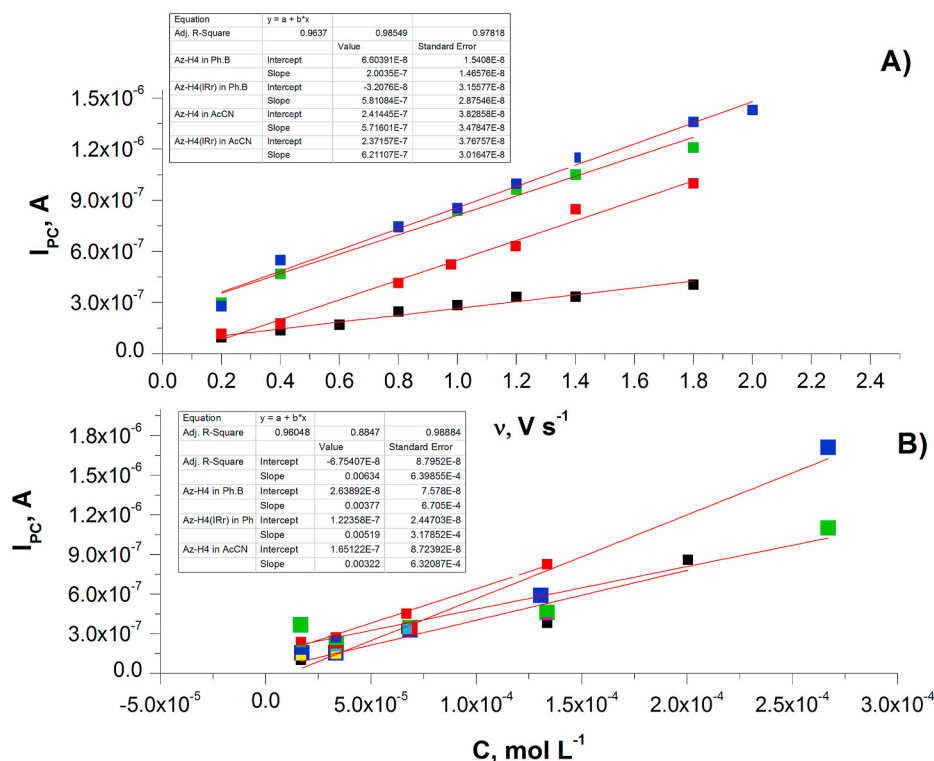


**Fig. 7.** (A) Plot of  $I_{pc}$  vs.  $v$  ( $V s^{-1}$ ) at  $6.681 \times 10^{-5}$  mol L<sup>-1</sup> Az-H4 and (B) Plot of  $\log I_{pc}$  vs.  $C$  (mol L<sup>-1</sup>) for azo peptide compound before and after 90 min UV illumination at  $\lambda = 365$  nm and different solvents: phosphate buffer solution (pH 6.86) and AcCN at HMDE electrode.

to investigate their influence on the physicochemical properties of the compound in case of their presence in biological fluids. Therefore, a qualitative assessment of the effect of metal ions such as  $\text{Cu}^{2+}$ ,  $\text{Ni}^{2+}$  and  $\text{Zn}^{2+}$  on the type of fluorescence spectrum was performed. As can be seen from Fig. 6, the fluorescence spectrum of the solution in the presence of copper ions is not significantly affected by the presence of the metal ion. A slight hyperchromic effect is only observed which metal was added (Fig. 6). In opposite to the mentioned above addition of Ni and Zn ions, the fluorescent bands of Az-H4 are very low and shifted to the red region. This leads to the conclusion that these ions affect the spectral properties of the compound by quenching their fluorescence. The change in the intensity of the analytical signals can be related to the performance of complex-forming processes in the solution and deserves in-depth future research. The photochromic behavior of the Az-H4 shows promising results for a future application for example as a chemosensor in photodynamic therapy.

In the next section, we show some structure-active characterization and *in vivo* biological experiments related to the *trans* (E) and *cis* (Z) isomers.

### 3.3. Electrochemistry

As for the study of the potential biological action of a compound, it is important to study electron and proton transfer processes to get a clearer idea of their structural activity. Proton-coupled electron transfer (PCET) reactions and the transport of protons are involved in a variety of biochemical processes, for example, in the respiratory chain, photosynthesis and protein functioning [60]. Therefore the electrochemical parameters as diffusion coefficient and heterogenous rate constant of Az-H4 and the same compound after 90 min UV illumination at 365 nm were calculated applying cyclic voltamperometry at HMDE (handing mercury drop electrode) in solutions with different dielectric constants: phosphate buffer solution (pH 6.86); DMSO and AcCN. The all voltamperograms were recorded in a potential windows from 0.2 to  $-1.4$  V (Fig. 6). The voltammetric characterizations are given in Table 2. The blank voltammogram of the solvent in the potential window of HMDE strengthened the belief that the oxidation signals are of compounds: Az-H4 and Az-H4(IRr) only. In the literature, information on the electrochemical behavior of azopeptide compounds and their conformational states is scarce. In our previous work were discussed the electrochemical properties of azobenzene-containing VV-hemorphin-5 analogue and confirmed the fact that the E $\rightarrow$ Z transformation changes the electrochemical behavior of the compound by altering the reactivity of the redox-active azo group [38]. The azo center in *cis* (Z)-isomeric form surrounded by symmetrically arranged peptide fragments was spatially inhibited, which is why, together with the bulky molecule it was a prerequisite for poorer diffusion through the electrode space. To evaluate the transfer of particles to and from the electrode space of the azo “-N=N-“ component in a smaller and mobile azopeptide molecule, the polarograms were recorded in three electrolyte media at a mercury working electrode. In an aprotic polar solvent such as DMSO and analyte concentration from  $1.00$  to  $7.00 \times 10^{-5}$  mol L $^{-1}$  no electrochemical electron transfer to the electrode space was observed and the voltammogram followed the type of the electrolyte signal. Even the addition of tetra butylammonium persulfate as an electrolyte salt in the organic solution does not provoke electronic exchange. The presence of cathodic and anodic signals of the compound was found to be clearly more favorable for electron exchange in the electrolytes: phosphate buffer solution (pH 6.86) and acetonitrile. One can see that in the both phosphatic buffer and AcCN solution a well formed cathodic peak localized at lower potential is observed which can be attributed to the reduction of the -N=N- group to -NH-NH- (Fig. 6-A, C). A second one peak is appeared at potential  $\approx -0.800$  V in the protonic solution which could be related to the peptide fragment (Fig. 6-A) [38,43]. The reversibility of the first peak in pH 6.86 can be assumed because one can see a difference from  $\approx 18$  mV provoked from peak potential difference:

**Table 3**

The equations of regression of the function of  $I_{PC,A} = f(\nu^{1/2})$ , mV s $^{-1}$  of Az-H4 before and after (Az-H4 (IRr)) UV irradiated with  $\lambda = 365$  nm at concentration  $6.681 \times 10^{-5}$  mol L $^{-1}$  in different electrolyte media and values of diffusion coefficient; HMDE electrode (with electrode area,  $A = 0.030$  cm $^2$ ).

Compound/electrolyte	Equation of regression	R $^2$	$D \times 10^{-3}$ cm $^2$ s $^{-1}$
Az-H4/Ph.buffer (pH 6.86)	$I_{PC} = -8.06.10^{-8} + 3.61.10^{-7} \times (\nu^{1/2})$	0.991	0.805
Az-H4(IRr)/Ph.buffer (pH 6.86)	$I_{PC} = -4.19.10^{-7} + 1.01.10^{-6} \times (\nu^{1/2})$	0.989	1.36
Az-H4/AcCN	$I_{PC} = -1.65.10^{-7} + 1.02.10^{-6} \times (\nu^{1/2})$	0.990	1.36
Az-H4(IRr)/AcCN	$I_{PC} = -2.48.10^{-7} + 1.17.10^{-6} \times (\nu^{1/2})$	0.995	1.47

R-coefficient of regression; n-number of electron number of electrons transferred in the redox event.

$\Delta E_p = E_{pc} - E_{pc}/2$  [38] as well the ratio of peak heights:  $I_{pc}/I_{pa}$  - greater than one which means that the reduction could be attributed to reversible; the current increased with the increase in scan rate from 0.2 to 2.00 Vs $^{-1}$  (Fig. 7) with the cathodic peak potential shifting to the more negative potentials. The same can be concluded for the behavior of the electrochemical reduction of the azo group in acetonitrile with small differences (Fig. 6-B and Fig. 6-D):  $\Delta E_p = E_{pc} - E_{pc}/2 \approx 25$  mV;  $I_{pc}/I_{pa}$  greater than one; reversible electrochemical process; the current increased with the increase in scan rate from 0.2 to 2.00 Vs $^{-1}$  without shifting. That is meaning the rate of electron transfer between the working electrode and the solution redox species is lower than the rate of transfer of the azo-peptide to the electrode space. Different electrochemical behavior of the azo compound was observed after *trans* (E) $\rightarrow$ *cis* (Z) transformation of azo-peptide molecule. The cyclic voltammograms of the *trans*(E)- and *cis*(Z)- isomers of Az-H4 on HMDE at different concentration and electrolyte media are shown in Fig. 6-A and B. As a result of the performed isomerization and the resulting spatial disturbances, the second peak in the phosphate buffer medium refers to the reduction of the peptide part disappears as the intensity of the current peak increases, which increases the sensitivity of the determination (Fig. 6-A). In an acetonitrile medium, a smaller increase in the signal intensity of the *cis* (Z)- form was observed compared to the current height in the proton medium without changing the condition for the signal appearing (at  $\approx 0.550$  V). Thus, as a result of the obtained data can be concluded that both the type of solvent (electrolyte medium) and the isomeric form of the Az-H4 affect its electrochemical properties as follows: from completely inactive in the aprotic DMSO solvent to the appearance of a well-formed azo component peak in acetonitrile and a highly intense current signal in phosphate buffer with the most pronounced properties in Az-H4(IRr). Voltammograms shown in Fig. 6-A and Fig. 6-B clearly depict that  $I_{pc}$  vary linearly with the escalation in concentration at Az-H4 and Az-H4 (IRr) which indicates that radical anion reduction product of the investigated compound, is adsorbed on the mercury electrode. A adsorption controlled process of the Az-H4(IRr) compound in phosphatic buffer solution is proved from potential shifting toward more negative values with increasing of the azopeptide concentration. On Fig. 6-B is also showed a proportional increase in the signal with increasing peptide concentration in AcCN solution without being followed by a shift in the potential peak. The regression equations plot of  $I_{pc}$ , A vs C, mol L $^{-1}$  are given in Figs. 7 and 8. From the slope of regression equations obtained using the formula  $I_{pc} = nFAC\omega_k$  (Reinmuth expression) the heterogeneous electron transfer rate constants were calculated (Table 2) and the obtained values predict the reduction process of the azo group to be quasi-reversible [38]. The number of electron transfer in electrochemical reaction for the reversible systems Az-H4 and Az-H4(IRr) is equal of 1 and was calculated from the equation:  $\Delta E_p (E_{pc} - E_{pa}) = 59/n$  mV.

Scan rate effect was also evaluated at scan rate from 0.2 to 2.00 Vs $^{-1}$

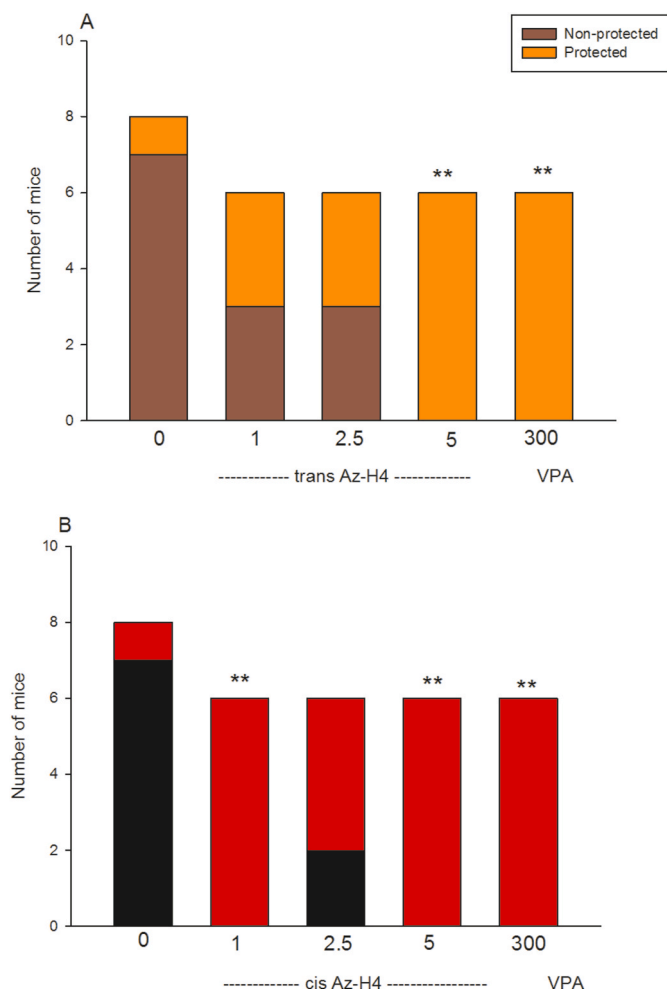


**Fig. 8.** Comparative analysis of the anticonvulsant activities of cis/trans-Az-H4 analogues in the 6-Hz test in mice. Valproate (VPA) is used as a positive control. Fisher exact test: \*\*\*P < 0.01 compared to controls.

**Table 4**  
Anticonvulsant activity of *trans* Az-H4 and *cis* Az-H4 in MES test in mice.

Drug	Dose ( <i>trans/cis</i> Az-H4 in µg/mouse) (Phenytoin in mg/kg)	No. of animals protected/No. of animals tested	% Protection	% Mortality
Control	0	0/8	0	67
<i>trans</i> Az-H4	1	2/6	33	0
	2.5	5/6	83	16
	5	4/6	67	0
	30	6/6	100	0
<i>cis</i> Az-H4	1	5/6	83	16
	2.5	4/6	67	0
	5	2/6	33	50
	30	6/6	100	0

In the rotarod test, the novel analogue of azobenzene-containing hemorphin-4 did not display neurotoxicity at the maximum dose of 5 µg/mouse.

(Fig.6-C, Fig. 6-D, Fig. 7). The plot of peak current versus scan rate gave a straight lines for two isomers of Az-H4, which is expressed for an ideal reaction of diffusion controlled electrode process for the azo-peptide compound (Fig.7).

The diffusion coefficients ( $D$ ,  $\text{cm}^2 \text{s}^{-1}$ ) if we assumed that the systems are reversible are listed in Table 3 and were determined by the equations of regression of the function of  $I_{p,c}A = f(\nu^{1/2})$ ,  $\text{mV s}^{-1}$  using:  $I_p = 268$ ,

$600 n^{3/2}AD^{1/2}C\nu^{1/2}$  validate at 25 °C (Randles-Secik [38]),  $I_p$  = current maximum in Amps;  $n$ : number of electrons transferred in the redox event;  $A$ -electrode area in  $\text{cm}^2$ ;  $F$ : Faraday Constant,  $\text{C mol}^{-1}$ ;  $C$  = concentration in  $\text{mol/ml}$ ;  $\nu$  = scan rate in  $\text{Vs}^{-1}$ ;  $R$ : Gas constant,  $\text{K}^{-1} \text{mol}^{-1}$  and temperature  $T$  in K. From the obtained values of ( $D$ ) coefficients of both Az-H4 and Az-H4(IRr) we can conclude that the change in the isomeric states does not affect the value of the diffusion coefficient, ie the movement/diffusion of the molecule from the inside of the solution to the surface of the electrode space does not depend on its spatial structure change.

In the next section we show the some *in vivo* biological experiments related to the *trans* (E) and *cis* (Z) isomers. The electrochemical technique allows being used to control of depletion/action of the pharmacophore in biological tissue.

### 3.4. Pharmacology

Screening for anticonvulsant activity and neurotoxicity of novel analogue of azobenzene-containing hemorphin-4.

The anticonvulsant activity of the novel analogue of azobenzene-containing hemorphin-4 was evaluated according to the guidelines of the Antiepileptic Drug Development Program (ADD) of the National Institutes of Health (USA) [50]. The two tests, 6-Hz and MES were applied for preliminary screening of anticonvulsant activity in parallel with neurotoxicity assessment through the test for minimal motor impairment (rotarod). Valproate (VPA) was used as a positive control in the 6-Hz test and Phenytoin in the MES test. The results are shown in Fig. 8 (6-Hz test) and Table 4 (MES test).

The drugs with anticonvulsant activity in the 6-Hz test are suggested as being effective against drug-resistant epilepsy and potency to modify sodium channels [51]. The *cis*-Az-H4 isomer exhibited higher activity than the *trans*-Az-H4 against the psychomotor seizures. It demonstrated 100% protection at the lowest dose of 1 µg/mouse used which effect was comparable to the positive control VPA (Fisher exact test:  $P < 0.01$  vs control) (Fig. 8). Also, at the highest dose of 5 µg, both the *cis*-Az-H4 and *trans*-Az-H4 showed 100% protection against the 6-Hz psychomotor seizures (Fisher exact test:  $P < 0.01$  vs control).

Like in the 6-Hz test, the *cis*-Az-H4 exhibited potency to suppress tonic-clonic seizures in the MES test with 83% protection vs 100 protection for the positive control Phenytoin (Table 4). Further, higher doses of this compound showed the decreasing ability of the peptide analogue to prevent the seizure spread.

## 4. Conclusion

In summary, the influence of *cis*(Z)- and *trans*(E)- isomers of newly synthesized biopeptide bearing azobenzene to the N-side chain of hemorphin-4 from the absorption, fluorescence, and electrochemical energy have been investigated in different environments. Generally, the properties of the photoswitchable Az-H4 upon long-wavelength UV light as *trans* (E) and *cis* (Z) isomers depends on the type of solvent and is observed as a decrease in the intensity of the spectral lines - absorption and emission and an increase in voltammetric current intensity which confirms the performance of intramolecular energy transitions mainly influenced by the transformation of *trans* into *cis* isomerization. The biological properties of the two isomers were also studied. The photo-physical properties showed structure-activity relation of  $E \rightarrow Z$  activated by long-wavelength light at 365 nm. The Z-isomer of the azopeptide has pronounced anticonvulsant activity in the 6 Hz test for psychomotor seizures where the compound showed potency in the first tested dose with 83% protection vs 100 protection for the positive control Phenytoin.

### Ethical statement

All procedures were performed in agreement with the European

Communities Council Directive 2010/63/EU. The experimental design was approved by the Institutional Ethics Committee. There are no human participants.

### Declaration of competing interest

The authors declare that they have no known competing financial interests or personal relationships that could have appeared to influence the work reported in this paper.

### Acknowledgements

This work was financial supported by the Bulgarian National Scientific Fund project ДН 18/5 “Novel azo materials and application of their photophysical properties as reversible optical storage devices” of the Ministry of Education and Science, Bulgaria.

### References

- Moon KS, Kim HJ, Lee E, Lee M. Self-assembly of T-shaped aromatic amphiphiles into stimulus-responsive nanofibers. *Angew Chem Int Ed* 2007;46:6807–10.
- Chockalingam K, Blenner M, Banta S. Design and application of stimulus-responsive peptide systems. *Protein Eng Des Sel* 2007;20:155–61.
- Shah NH, Kirshenbaum K. Photoresponsive peptid oligomers bearing azobenzene side chains. *Org Biomol Chem* 2008;6:2516–21.
- Yujie Tu, Yeqing Yu, Zhibiao Zhou, Sheng Xie, Bicheng Yao, Shujuan Guan, Bo Situ, Yong Liu, Kwok Ryan TK, Lam Jacky WY, Sijie Chen, Xuhui Huang, Zebing Zeng, Ben Zhong Tang. Specific and quantitative detection of albumin in biological fluids by tetrazolate-functionalized water-soluble AIEgens. *ACS Appl Mater Interfaces* 2019;29619–29. 11.
- Mart RJ, Allemann RK. Azobenzene photocontrol of peptides and proteins. *Chem Commun* 2016;52:12262–77.
- Szymanski W, Beierle JM, Kistemaker HA, Velema WA, Feringa BL. Reversible photocontrol of biological systems by the incorporation of molecular photoswitches. *Chem Rev* 2013;113:6114–78.
- Goodman M, Falxa ML. Conformational aspects of polypeptide structure. XXIII. Photoisomerization of azoaromatic polypeptides. *J Am Chem Soc* 1967;89:3863–7.
- Goodman M, Kossoy A. Conformational aspects of polypeptide structure. XIX. Azoaromatic side-chain effects 1. 2. *J Am Chem Soc* 1966;88:5010–5.
- Concilio S, Sessa L, Petrone AM, Porta A, Diana R, Iannelli P, Piotta S. Structure modification of an active azo-compound as a route to new antimicrobial compounds. *Molecules* 2017;22:875.
- Piotta S, Trapani A, Bianchino E, Ibarguren M, López DJ, Busquets X, Concilio S. The effect of hydroxylated fatty acid-containing phospholipids in the remodeling of lipid membranes. *Biochim Biophys Acta Biomembr* 2014;1838:1509–17.
- Yager KG, Barrett CJ. Novel photo-switching using azobenzene functional materials. *J Photochem Photobiol, A* 2006;182:250–61.
- Beharry AA, Woolley GA. Azobenzene photoswitches for biomolecules. *Chem Soc Rev* 2011;40:4422–37.
- Banghart M, Borges K, Isacoff E, Trauner D, Kramer RH. Light-activated ion channels for remote control of neuronal firing. *Nat Neurosci* 2004;7:1381–6.
- Ochi R, Perur N, Yoshida K, Tamaoki N. Fast thermal cis–trans isomerization depending on pH and metal ions of water-soluble azobenzene derivatives containing a phosphate group. *Tetrahedron* 2015;71:3500–6.
- Fitz J, Mammanna A. Spectroscopic study of the pH dependence of the optical properties of a water-soluble molecular photo-switch. *Spectrochim Acta Mol Biomol Spectrosc* 2020;227:117576.
- Muramatsu S, Kinbara K, Taguchi H, Ishii N, Aida T. Semibiological molecular machine with an implemented “AND” logic gate for regulation of protein folding. *J Am Chem Soc* 2006;128:3764–9.
- Izquierdo-Serra M, Gascon-Moya M, Hirtz JJ, Pittolo S, Poskanzer KE, Ferrer E, et al. Two-photon neuronal and astrocytic stimulation with azobenzene-based photoswitches. *J Am Chem Soc* 2014;136:8693–701.
- Momotake A, Arai T. A new class of azobenzene chelators for Mg<sup>2+</sup> and Ca<sup>2+</sup> in buffer at physiological pH. *Tetrahedron Lett* 2003;44:7277–80.
- Perur N, Yahara M, Kamei T, Tamaoki N. A non-nucleoside triphosphate for powering kinesin-microtubule motility with photo-tunable velocity. *Chem Commun* 2013;49:9935–7.
- Diana R, Caruso U, Tuzi A, Panunzi B. A Highly Water-soluble fluorescent and colorimetric pH probe. *Crystals* 2020;10:83.
- Pieron O, Fissi A. New trends in photobiology: Synthetic photochromic polypeptides: possible models for photoregulation in biology. *J Photochem Photobiol B: Biol* 1992;12:125–40.
- Rovero P, Pegoraro S, Viganò S, Amato C, Vaccari L, et al. Solid-phase synthesis and dimerization of an azobenzene-containing peptide as photoisomerizable proteinase inhibitor. *Lett Pept Sci* 1995;2:27–32.
- Ch Renner, Moroder L. Azobenzene as conformational switchin model peptides. *Chembiochem* 2006;7:868–78.
- Caruso U, Panunzi B, Diana R, Concilio S, Sessa L, Shikler R, Nabha S, Tuzi A, Piotta S. AIE/ACQ effects in two DR/NIR emitters: a structural and DFT comparative analysis. *Molecules* 2018;23:1947.
- Virgili T, Forni A, Cariati E, Pasini D, Botta C. Direct evidence of torsional motion in an aggregation-induced emissive chromophore. *J Phys Chem* 2013;117:27161–6.
- Jin Y, Huang Y, Yang H, Liu G, Zhao R. A peptide-based pH-sensitive drug delivery system for targeted ablation of cancer cells. *Chem Commun* 2015;51:14454–7.
- Wang P, Wu J, Su P, Shan C, Zhou P, et al. A novel fluorescent chemosensor based on tetra-peptides for detecting zinc ions in aqueous solutions and live cells. *J Mater Chem B* 2016;4:4526–33.
- Zhang M, Li M, Zhao Q, Li F, Zhang D, Zhang J, et al. Novel Y-type two-photon active fluorophore: synthesis and application in fluorescent sensor for cysteine and homocysteine. *Tetrahedron Lett* 2007;48:2329–33.
- Tang B, Yu F, Li P, Tong L, Duan X, et al. A near-infrared neutral pH fluorescent probe for monitoring minor pH changes: imaging in living HepG2 and HL-7702 cells. *J Am Chem Soc* 2009;131:3016–23.
- Wang Y, Tang B, Zhang S. A visible colorimetric pH sensitive chemosensor based on azo dye of benzophenone. *Dyes Pigments* 2011;91:294–7.
- Thirupathi P, Lee KH. A new peptidyl fluorescent chemosensors for the selective detection of mercury ions based on tetrapeptide. *Bioorg Med Chem* 2013;21:7964–70.
- Kim JM, Lohani CR, Neupane LN, Choi Y, Lee KH. Highly sensitive turn-on detection of Ag<sup>+</sup> in aqueous solution and live cells with a symmetric fluorescent peptide. *Chem Commun* 2012;48:3012–4.
- Li Y, Li L, Pu X, Ma G, Wang E, Kong J, et al. Synthesis of a ratiometric fluorescent peptide sensor for the highly selective detection of Cd<sup>2+</sup>. *Bioorg Med Chem Lett* 2012;22:4014–7.
- Gomes I, Dale CS, Casten K, Geigler MA, Gozzo FC, Ferro ES, et al. Hemoglobin-derived peptides as novel type of bioactive signaling molecules. *AAPS J* 2010;12:658–69.
- Ferro ES, Rioli V, Castro LM, Fricker LD. Intracellular peptides: from discovery to application. *EuPA Open Proteom* 2014;3:143–51.
- Schechter AN. Hemoglobin research and the origins of molecular medicine. *Blood* 2008;112:3927–38.
- Brantl V, Gramsch C, Lottspeich F, Mertz R, Jager KH. Novel opioid peptides derived from hemoglobin: hemorphins. *Eur J Pharmacol* 1986;125:309–10.
- Todorov PT, Peneva PN, Georgieva SI, Tchekalarova J, Vitkova V, et al. Synthesis, characterization and anticonvulsant activity of new azobenzene-containing VV-hemorphin-5 bio photoswitch. *Amino Acids* 2019;51:549–63.
- Todorov P, Peneva P, Pechlivanova D, Georgieva S, Dzhabazova E. Synthesis, characterization and nociceptive screening of new VV-hemorphin-5 analogues. *Bioorg Med Chem Lett* 2018;28:3073–9.
- Todorov P, Peneva P, Tchekalarova J, Georgieva S. Potential anticonvulsant activity of novel VV-hemorphin-7 analogues containing unnatural amino acids: synthesis and characterization. *Amino Acids* 2020;24:1–9.
- Todorov P, Peneva P, Tchekalarova J, Rangelov M, Georgieva S, Todorova N. Synthesis, characterization and anticonvulsant activity of new series of N-modified analogues of VV-hemorphin-5 with aminophosphonate moiety. *Amino Acids* 2019;51:1527–45.
- Todorov P, Rangelov M, Peneva P, Todorova N, Tchekalarova J. Anticonvulsant evaluation and docking analysis of VV-Hemorphin-5 analogues. *Drug Dev Res* 2019;80:425–37.
- Todorov P, Peneva P, Tchekalarova J, Georgieva S, Rangelov M, Todorova N. Structure–activity relationship study on new hemorphin-4 analogues containing steric restricted amino acids moiety for evaluation of their anticonvulsant activity. *Amino Acids* 2020;52:1375–90.
- Kaiser E, Colescott RL, Bossinger CD, Cook PI. Color test for detection of free terminal amino groups in the solid-phase synthesis of peptides. *Anal Biochem* 1970;34:595.
- Sarin VK, Kent SB, Tam JP, Merrifield RB. Quantitative monitoring of solid-phase peptide synthesis by the ninhydrin reaction. *Anal Biochem* 1981;117:147–57.
- Bandara HD, Basa PN, Yan J, Camire CE, MacDonald JC, et al. Systematic modulation of hydrogen bond donors in aminoazobenzene derivatives provides further evidence for the concerted inversion photoisomerization pathway. *Eur J Org Chem* 2013;4794–803. 2013.
- Ryu EH, Zhao Y. An amphiphilic molecular basket sensitive to both solvent changes and UV irradiation. *J Org Chem* 2006;71:9491–4.
- Haneda T, Kawano M, Kojima T, Fujita M. Thermo-to-Photo-Switching of the chromic behavior of salicylideneanilines by inclusion in a porous coordination network. *Angew Chem Int Ed* 2007;46:6643–5.
- Young DD, Deiters A. Photochemical control of biological processes. *Org Biomol Chem* 2007;5:999–1005.
- Krall RL, Penry JK, White BG, Kupferberg HJ, Swinyard EA. Antiepileptic drug development: II. Anticonvulsant drug screening. *Epilepsia* 1978;19:409–28.
- Potschka H. Animal models of drug-resistant epilepsy. *Epileptic Disord* 2012;14:226–34.
- Said Benkhaya. M'rabet Souad, Harfi Ahmed El. Classifications, properties, recent synthesis and applications of azo dyes. *Heliyon* 2020;6. e0327.
- Zhang C, Zhu Z, Zhang H. Mg-based amorphous alloys for decolorization of azo dyes. *Results in Physics* 2017;7:2054–6.
- Shankarling GS, Deshmukh PP, Joglekar AR. Process intensification in azo dyes. *Journal of Environmental Chemical Engineering* 2017;5:3302–8.
- Adochitei A, Dochioiu G. Rapid characterization of peptide secondary structure by ft-ir spectroscopy. *Rev Roum Chem* 2011;56:783–91.

- [56] Rusu E, Dorohoi D-O, Airinei A. Solvatochromic effects in the absorption spectra of some azobenzene compounds. *J Mol Struct* 2008;887:216–9.
- [57] Watkins AM, Craven TW, Renfrew PD, Arora PS, Bonneau R. Rotamer libraries for the high-resolution design of  $\beta$ -amino acid foldamers. *Structure* 2017;25:1771–80. e3.
- [58] Fornander LH, Feng B, Beke-Somfai T, Nordén B. UV transition moments of tyrosine. *J Phys Chem B* 2014;118:9247–57.
- [59] Yashchuk VM, VYu Kudrya, Levchenko SM, ZYu Tkachuk, Hovorun DM, Mel'nik VI, Vorob'yov VP, Klishevich GV. Optical response of the polynucleotides-proteins interaction. *Mol Cryst Liq Cryst* 2011;535:93–110.
- [60] Migliore A, Polizzi NF, Therien MJ, Beratan DN. Biochemistry and theory of proton-coupled electron transfer. *Chem Rev* 2014;114:3381–465.